International Journal of Engineering & Technology, 7 (4) (2018) 4866-4872

International Journal of Engineering & Technology

Website: www.sciencepubco.com/index.php/IJET
doi: 10.14419/ijet.v7i4.26071
Research paper

Computer vision performance metrics evaluation of object detection based on Haar-like, HOG and LBP features for scale-invariant lettuce leaf area calculation

Pocholo James Loresco [1] *, Argel Bandala [1], Alvin Culaba [2], Elmer Dadios [3]

[1] *Department of Electronics and Communications Engineering, De La Salle University, Manila Philippines*
[2] *Department of Mechanical Engineering, De La Salle University, Manila Philippines*
[3] *Department of Manufacturing Engineering and Management, De La Salle University, Manila Philippines*
**Corresponding author E-mail: pocholo_loresco@dlsu.edu.ph*

Abstract

Leaf area can be used as a growth parameter as such it increases as the stage of lettuce progresses. Consideration of scale invariance in estimating the area poses challenging machine vision problems in a smart farm setup. To address this, a marker with a known area is utilized for the system for normalizing area measurements. This study proposes an automated object detection (marker) using Viola-Jones algorithm that uses Haar-like, HOG and LBP features. Performances of the system using each feature at varying illuminations and distances are then compared. Based on the result of this study, the highest performance in general, based on accuracy, precision, and false positive rate is achieved using HOG features.

Keywords: *Haar-Like, HOG, LBP Features; Lettuce Leaf Area; Scale Invariance; Viola-Jones Algorithm.*

1. Introduction

Smart farming is an efficient use of resources while maintaining the optimum amount of harvest. This type of agricultural process requires a lot of monitoring specifically on the growth and development of the crops [1]. Growth analysis can account for plant parameters which entails measurements and allometric functions of obtaining estimates of parameters that describe growth [2]. Leaf area can be used as a growth parameter as such it increases as the stage of lettuce progresses. The leaf area when measured can be significant reference tool to predict photosynthetic primary production and characterize lettuce plant growth [3] [4].

Image processing method of measuring leaf area can be regarded as an efficient alternative to identify plant growth compared to other methods which are not only laborious and destructive but also expensive [5]. Existing literatures for lettuce plant growth monitoring using image processing have numerous inherent problems open to research. Machine vision problems with regards to lettuce growth monitoring remain a challenging task as such systems have required some degree of human intervention using a software for image processing [6] [7]. Consideration of light adaptability and scale invariance further make the machine vision problems more challenging. In fact, scale invariance is one of the most common machine vision limitations of existing literatures [8] [9].

To address scale invariance, a marker with a known area is utilized for the system for normalizing area measurements as seen in Figure 1. This marker will make the system to have the property of being invariant to scaling which is significant for accurate leaf area calculation.

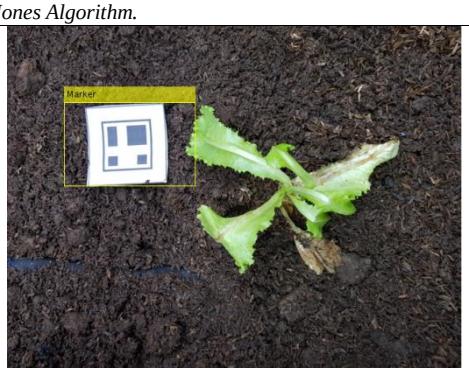


Fig. 1: Marker to Detect in Yellow Bounding Box.

The detection of the marker is a preliminary step to allow scale correction by determining the area of known component of the marker and relate it to the number of pixels. In this way a more accurate lettuce leaf area can be calculated from images taken at any given distance. The area of the black square (1.8 cm by 1.8 cm) component of the marker used in this research bounded by red outline shown in Figure 2 is 3.24 cm^2. This area would be related to the actual number of pixels of the reference component to produce a scaling factor given in area per pixel as shown in Equation 1. The scaling factor is multiplied to the number of pixels of segmented lettuce leaf to calculate the lettuce leaf area in cm^2.

Copyright © 2018 Pocholo James Loresco et al. This is an open access article distributed under the Creative Commons Attribution License, which permits unrestricted use, distribution, and reproduction in any medium, provided the original work is properly cited.

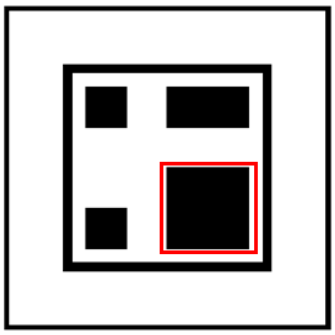


Fig. 2: Reference Component Bounded by Red Box.

The type of feature descriptors contributes significantly to the effectiveness of object detection [10]. This study determines which among the features Haar-like, Histogram of Gradients (HOG) and Local Binary Patterns (LBP) can be best used along with Viola-Jones Algorithm to detect the said marker for a scale-invariant method of calculation of lettuce leaf area. Computer vision metrics such as sensitivity, false positive rate, precision and accuracy are used to evaluate the performance for each feature at varying distances and illumination.

$$L = P\frac{3.24}{C} \quad (1)$$

Where L is actual lettuce area in sq. cm, P is actual pixel area and C is reference component pixel area

This paper consists of six sections arranged as follows. The first section introduces the research topic. The 2nd section discusses the object detection using Haar-like, HOG and LBP features. Section III and IV presents the experiment setup and the methodology used. Section V discusses the experimental results and its analysis. Lastly, section VI presents conclusions and future works.

2. Object detection by viola-jones

Object detection is the method of locating objects of interests within an image. One of the most commonly used technique for object detection is Viola and Jones algorithm for its high accuracy, low false positive detection rate and speed of detection. This efficiency of the method is due to three key components in Viola and Jones's technique which are computing integral picture, adaptive boosting, and cascading. However, to accurately identify a given object many features are needed. Thus, Viola-Jones classifier also used a boosted rejection cascade that incorporates multiple features and checks them in order of mostly likely to occur allowing unlikely regions of an image to be rejected early in computation [11]. Features that can be used along with Viola-Jones algorithm are presented on this section.

2.1. Haar features

Viola Jones method may use Haar wavelets which are digital image features. Figure 3 shows some example of Haar features.

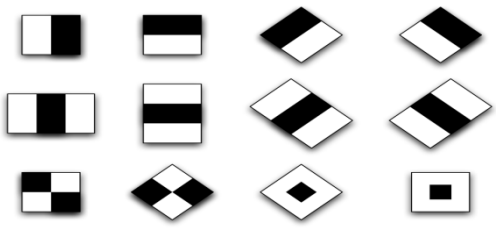


Fig. 3: Haar-Like Features [12].

Haar feature is determined by summing pixel intensity in adjacent rectangular regions of the detection area, then subtracting these sums in dark and bright regions. Viola-Jones use summed-area tables called integral images [13]. The sum of the rectangular areas can be computed using Equation 2. These differences are compared against learned threshold values to conclude whether the object appears in the region.

$$\text{sum} = I(C) + I(A) - I(B) - I(D) \quad (2)$$

Where A, B, C, D are edges plotted clockwise belonging to the integral image I

2.2. Histogram of oriented gradients (HOG)

Histogram of Oriented Gradients is a feature extraction based on the principle that the descriptors can be established by constructing histograms of local intensity gradients. To do this, the image is divided into smaller cells and a histogram of gradient directions or edge orientations weighted by the amplitude of the gradient [14]. Configurations of several cells form blocks as shown in Figure 4. The gradient is computed by convolution of the image with a first derivative mask. The components of horizontal and vertical gradients can then be computed using Equations 3 and 4. The amplitude of the gradient and its direction in terms of Θ can be calculated using Equation 5 and 6.

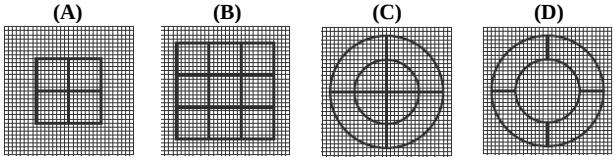


Fig. 4: Examples of Rectangular and Circular Blocks of Cells That May be Used in HOG Descriptors. (A-D) [14].

$$G_x = [1\ 0\ -1] * I(x,y) \quad (3)$$

$$G_y = [1\ 0\ -1]^T * I(x,y) \quad (4)$$

$$G = \sqrt{G_X^2 + G_Y^2} \quad (5)$$

$$\theta = \arctan\left(\frac{G_y}{G_x}\right) \quad (6)$$

2.3. Local binary patterns (LBP)

The LBP descriptor is based on a process of threshold the brightness from a center pixel gray level to its local neighborhood to form a binary pattern. Texture can be derived locally comparing a center pixel with pixel neighborhood consisting of several pixels P equally spaced points of distance R centered at the center pixel [15]. Examples are presented in Figure 6. The texture is described in Equation 7.

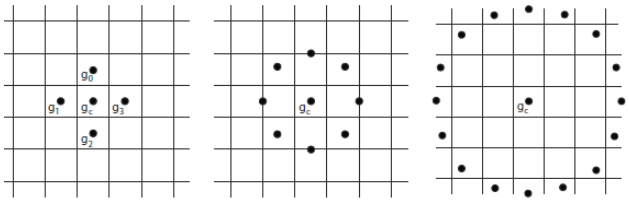


Fig. 6: Circularly Symmetric Neighborhoods for Different Values of P & R (A) P=4, R=1 (B) P=8, R=1.5 (C) P=16, R=3.0 [15].

$$T = t(g_c, g_0, g_1, \ldots, g_{P-1}) \quad (7)$$

Where g_c is the gray level of the central pixel and g_0, g_{P-1} are gray values of the neighborhood pixels. Assuming the coordinates of G_c are (0, 0), coordinates of the neighborhood pixels g_p are given by [−Rsin (2πp/P), Rcos (2πp/P)].

Mathematically, LBP can be expressed as shown in Equation 8:

$$LBP_{P,R} = \sum_{P=0}^{P-1} s(g_P - g_C)2^P \quad (8)$$

3. Experiment setup

The smart farm environmental chamber is designed to produce a maximum number of harvestable crops. The lighting system and temperature control systems automatically adjust depending on the stage of the crop being planted. The vision system is developed to determine the crop stage. The irrigation system automatically opens when the soil moisture of the plant beds decreases beyond the threshold. All these parameters are monitored everyday through Internet-of-Things.

3.1. Lettuce and leaf area

Loose-leaf lettuce was planted in the controlled environment chamber. It has three growth stages namely sowing, vegetative and harvest. The sowing stage or germination in nursery usually took 0-12 days. Then, the plant is transplanted and grown in the chamber until 21 days. Vegetative stage starts once the crop is transplanted. By this time, the crop is transferred in the environmental chamber where the lighting, water, temperature and NPK are controlled. Harvest stage happens between 45 - 65 days old of the lettuce [16].
Leaf area increases as the stage of lettuce progresses; thus, it can be used as a growth parameter. Canopy area calculated from the segmented lettuce images can be compared in the learned thresholds that indicate the lettuce growth whether there are sowing, vegetative, or harvest stage. Therefore, the accurate area determination determines the performance of such system.

3.2. Image capturing setup

The lettuce plants are assumed to be planted in soil by fours per plant box evenly spaced between rows and columns in a controlled environment chamber. Lettuce images were captured using a monocular camera positioned inside the chamber such as shown in Figure 7. To lessen ocular distortion of the images captured, the camera zoom ratio was fixed to 1:1. LED lights were used as a source of white light and no direct sunlight was allowed inside the chamber to maintain the quality of the taken images



Fig. 7: Image Capturing Setup.

A positioned camera taken top view of the canopy between 2 feet, 3 feet and 5 feet of altitude away from the lettuce. Variation on illumination was taken into consideration on the experimentation. Four variation of light illumination were considered with Photosynthetically Active Radiation (PAR) values as 92 µmol $m^{-2}s^{-1}$, 44 µmol $m^{-2}s^{-1}$, 7µmol $m^{-2}s^{-1}$, 3 µmol $m^{-2}s^{-1}$ measured from a Vernier PAR sensor.

4. Machine learning methodology

Figure 8 illustrates the block diagram of the machine learning methodology of the research. The methodology for marker detection composed of training phase and testing phase. The learning method on this research was data-driven. Data sets were used to train and test the system.

In the first part, lettuce images with or without markers were captured. These images were used as training as well as test images for the system. Image pre-processing improved the input lettuce images, enhancing the important image features before feature extraction. This included image enhancement such as histogram equalization and median filtering. Next was the extraction of Haar-like, HOG and LBP features out of the image that were used to set up the cascade object detector. Representations from these extracted features were used to build the framework for training and creating the XMLs for the object detector by Viola-Jones algorithm. There were three XMLs created by the training corresponding to Haar-like, HOG and LBP features.

Training was followed by testing to validate the results. In the testing phase, since the system has sufficient training pairs, the system therefore was able to detect the marker when new inputs were introduced.

4.1. Training

Training the object detection system requires positive and negative images. Lettuce images were collected, and positive samples and negative were manually created. Positive samples contain image object (marker) to be detected which were manually specified by bounding box on the regions of interest (ROIs) as indicated in Figure 9. Lettuce images, that do not contain objects of interest (marker) such as the lettuce image shown in Figure 10 were captured using the camera. Negative samples should contain the backgrounds associated with the object to be detected such as the marker for the smart farm setup.

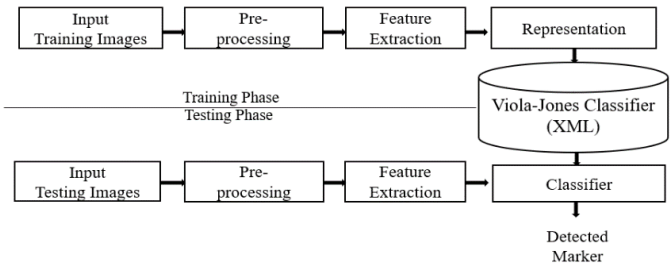


Fig. 8: Development Phases of the System.

The cascade classifier consists of stages. Using sliding window, each stage of classifier defined the specific region as either positive or negative. Positive means that marker of was found while negative indicates no marker was found. Whenever the region was found to be negative, the classification was said to be complete and the detector would slide to the next window. On the other hand, when the region was found to be positive, the classifier would pass the region to the next stage. The system would report that a marker was found at the current window when the final stage labeled the region as positive.

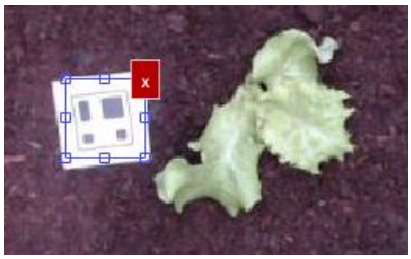


Fig. 9: Specifying the Region of Interest to Create Positive Samples.



Fig. 10: A Negative Sample.

The training of each new stage was preceded first by the function running the detector comprised of the stages already trained on the negative images which identified false positives. Thus, each new stage corrected itself by the mistakes of the previous stages. Increasing the stages decreased the overall false positive rate, however made the generation of negative samples more difficult.

Several parameters were considered in the training. These parameters were training size, number of cascade stages, false positive rate and feature type as shown in Table 1. The methodology trained a 1000-stage detector from a small training set of 134 images using Haar-like, HOG and LBP features. Most often, an accurate detector requires thousands of positive samples and negative images, however due to the limited available images limitations brought by the number of images was compensated by adjusting the number of stages and setting a lower false positive rate (FPR) for each stage. Thus, a true positive rate of 0.999 and a false positive rate of 0.001 were used in the study. The cascade object detector was trained using Haar-like, HOG and LBP features and stored as XML. For fair comparison, same training dataset and test dataset were used for each feature.

Table 1: Training Parameters

Training parameters	Value
No. of positive images	134
No. of negative images	134
No. of stages	1000
False positive rate	0.001
True positive rate	0.999

4.2. Testing phase

Each classifier was tested by running it on a set of positive and negative images. Training was followed by testing to assess the performance of the system. Test images were uploaded on the system. The methodology detected objects in images which may be marker or non-marker. The trained detector then used a Viola and Jones cascade classifier and sliding window technique to detect regions that contain the marker using the XML file saved on the system. The XML file contained codes transformed from marker images. Bounding box were drawn to the marker image to indicate and verify detection.

The proposed methodology is evaluated for different altitudes where the lettuce images where captured to test its effectiveness in addressing scale invariance. Light illumination was also changed to check its effect on the performance of the marker detection for each feature. Sensitivity, specificity, false positive rate, precision and accuracy in Equations (9) to (12) are statistical evaluation criteria of the performance of the marker detection [17].

$$\text{sensitivity} = \frac{TP}{TP + FN} \tag{9}$$

$$\text{precision} = \frac{TP}{TP + FP} \tag{10}$$

$$\text{accuracy} = \frac{TP + TN}{TP + TN + FP + FN} \tag{11}$$

$$\text{false positive rate} = \frac{FP}{FP + TN} \tag{12}$$

Where TP true positive, correctly identified markers, FP false positive, incorrectly identified markers TN true negative, correctly identified non-markers and FN false negative, incorrectly identified non-markers.

5. Discussion and analysis of results

This section presents the results of the research. Haar-Viola Jones, HOG-Viola Jones and LBP-Viola Jones methods has been implemented on 170 images to detect the markers. An example of detected marker with bounding box for each feature Haar-like, HOG and LBP are shown in Figures 11 to 13.



Fig. 11: Marker Detection Using Haar-Like Features with Marker Detected Bounded by Green Box.



Fig. 12: Marker Detection Using HOG Features with Marker Detected Bounded by Red Box.



Fig. 13: Marker Detection Using LBP Features with Marker Detected Bounded by Cyan Box.

Illumination was varied to test the methodologies. Ninety (90) images were used in this experiment. Sample results are shown in Figure 14. Results are shown in Tables 2 to 4. Optimal values for each computer vision metrics are shown in bold letters. Note that the numbers 1 to 4 corresponds to: 1-darkest up to 4-brightest, with

PAR values as 1: 3 µmol $m^{-2}s^{-1}$, 2: 7µmol $m^{-2}s^{-1}$, 3: 44 µmol $m^{-2}s^{-1}$ and 4: 92 µmol $m^{-2}s^{-1}$.

In various illuminations, LBP has the highest average sensitivity while HOG has the highest average specificity, precision, and accuracy. HOG has also obtained the favorable lowest average false positive rate for marker detection. Graphs for each vision metric at increasing illumination are shown in Figures 15 to 18.

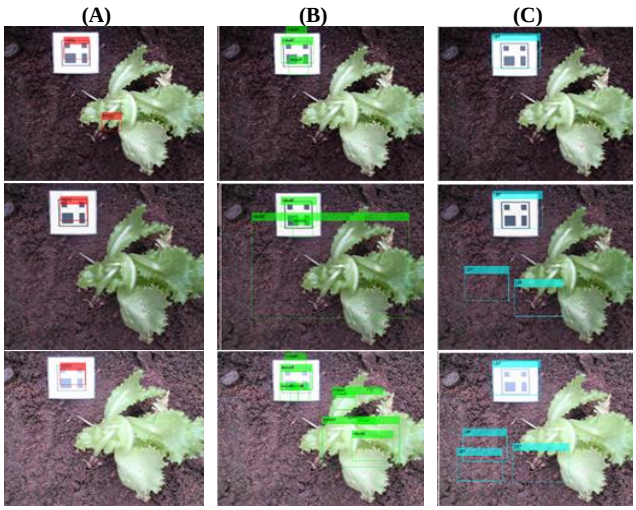


Fig. 14: Marker Detected at Varying Illumination (A) HOG (B) Haar (C) LBP.

Table 2: Evaluation Metrics for Haar at Varying Illumination

	Sensitivity	FPR	Precision	Accuracy
1	0.209302	0.936170	0.169811	0.133333
2	0.188679	0.985507	0.128205	0.090163
3	0.275000	0.913043	0.207547	0.174418
4	0.211538	0.985915	0.135802	0.097560
Ave.	0.221130	0.955159	0.160341	0.123869

Table 3: Evaluation Metrics for HOG at Varying Illumination

	Sensitivity	FPR	Precision	Accuracy
1	0.310344	0.714285	0.310344	0.298245
2	0.321428	0.703704	0.321428	0.309090
3	0.321428	0.826086	0.321428	0.254901
4	0.642857	0.312500	0.642857	0.666666
Ave.	0.399014	0.639144	0.399014	0.382226

Table 4: Evaluation Metrics for LBP at Varying Illumination

	Sensitivity	FPR	Precision	Accuracy
1	0.428571	0.846153	0.290322	0.276595
2	0.571428	0.826086	0.387096	0.363636
3	0.391304	0.840000	0.300000	0.270833
4	0.428571	0.826086	0.321428	0.295454
Ave.	0.454968	0.834581	0.324711	0.301629

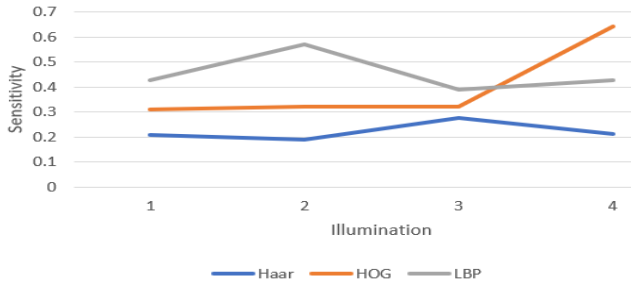


Fig. 15: Sensitivity at Increasing Illumination.

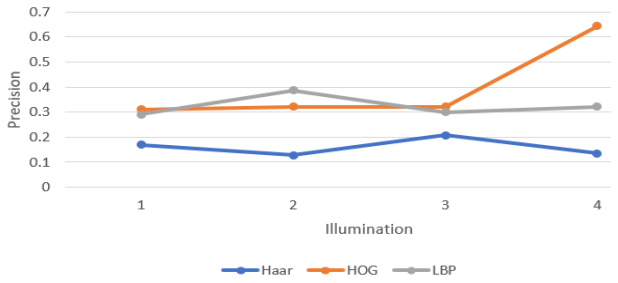


Fig. 16: Precision at Increasing Illumination.

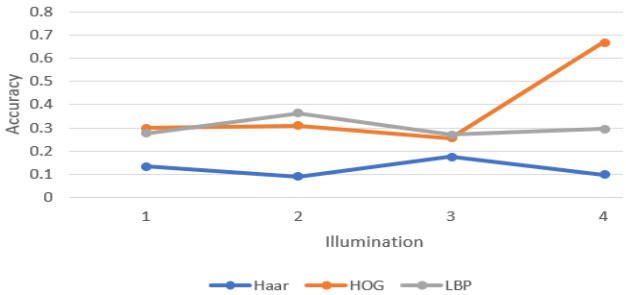


Fig. 17: Accuracy at Increasing Illumination.

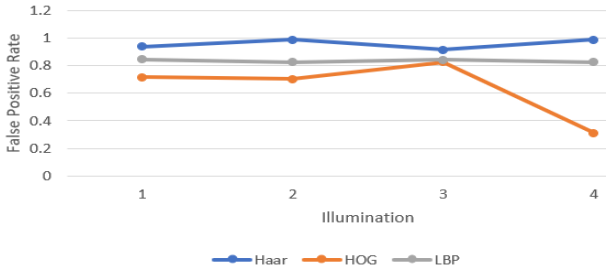


Fig. 18: False Positive Rate at Increasing Illumination.

Both Haar-like and LBP have a pattern of an initial increasing trend for precision, sensitivity, specificity and accuracy and reach a certain maximum value then went down again for brighter illumination. On the other hand, HOG feature offered a more consistent increasing trend for precision, sensitivity, specificity and accuracy while decreasing trend for false positive rate as the illumination increased.

Variation in heights of capture in testing the methodologies was also considered. This is done with a constant illumination. A maximum height of 5 feet was considered for placement of camera so that the images captured encompasses one whole plant box such as shown in Figure 7. The illumination is set to at 92 µmol $m^{-2}s^{-1}$ measured 1 foot from a PAR sensor. The results are shown in Tables 5 to 7.

In various altitudes, HOG performed the best for marker detection in terms of sensitivity, specificity, false positive rate, precision and accuracy. Graphs for each vision metric at increasing capture height are shown in Figures 19 to 22.

Table 5: Evaluation Metrics for Haar at Varying Heights

Distance	Sensitivity	FPR	Precision	Accuracy
1 foot	0.270270	0.925000	0.212765	0.168831
3 feet	0.263157	0.926829	0.208333	0.164556
5 feet	0.344827	0.906250	0.256410	0.213114
Ave.	0.292751	0.919359	0.225836	0.182167

Table 6: Evaluation Metrics for HOG at Varying Heights

Distance	Sensitivity	FPR	Precision	Accuracy
1 foot	0.400000	0.892857	0.285714	0.245283
3 feet	0.400000	0.892857	0.285714	0.245283
5 feet	0.370370	0.900000	0.270270	0.228070
Ave.	0.390123	0.895238	0.280566	0.239545

Table 7: Evaluation Metrics for LBP at Varying Heights

Distance	Sensitivity	FPR	Precision	Accuracy
1 foot	0.344827	0.906250	0.256410	0.213114
3 feet	0.312500	0.914285	0.238095	0.194029
5 feet	0.269230	0.906250	0.194444	0.172413
Ave.	0.308852	0.908928	0.229649	0.193186

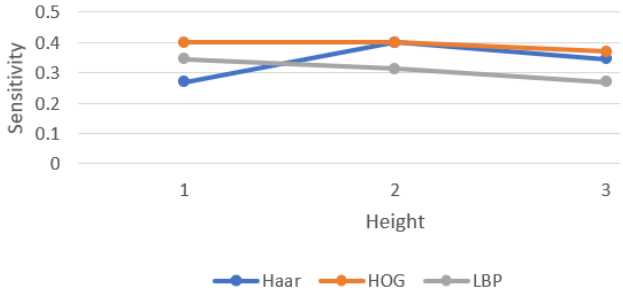


Fig. 19: Sensitivity at Increasing Capture Height.

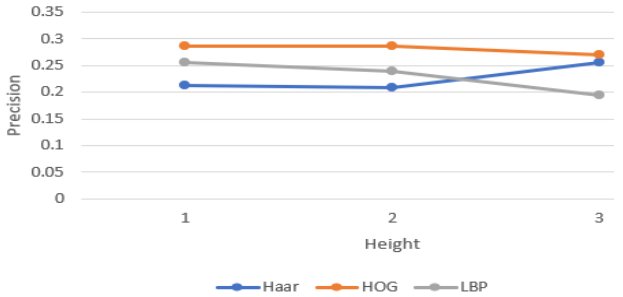


Fig. 20: Precision at Increasing Capture Height.

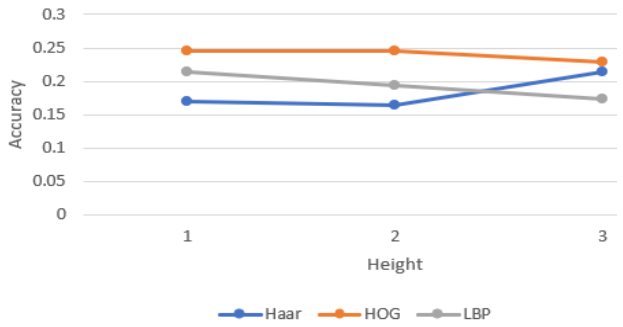


Fig. 21: Accuracy at Increasing Capture Height.

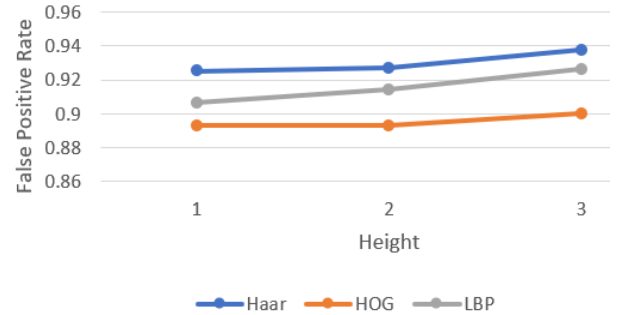


Fig. 22: False Positive Rate at Increasing Capture Height.

With altitude increasing, there is a downward trend for sensitivity, precision and accuracy for LBP and HOG while an inconsistent pattern of trend for Haar-like. False positive rate consistently increased for three features as the capture height increased.

As a whole, 170 images were analyzed with each feature using evaluation metrics based on the sensitivity, specificity, false positive rate precision and accuracy. The performances for each feature are summarized at Table 8. Based on the Table 8, HOG features performed best in object (marker) detection in general, based on accuracy, precision, and false positive rate. HOG also trained the object detection system at the lowest possible time.

Table 8: Performance Summary for Each Feature

	Feature type		
Evaluation metric	Haar	HOG	LBP
Sensitivity	0.238372	0.378787	0.389743
False positive rate	0.935406	0.772925	0.854077
Precision	0.173361	0.297619	0.276363
Accuracy	0.143044	0.297423	0.257009
Training Time (s)	91.426343	23.110529	31.756453

6. Conclusion

Scale invariance in finding leaf area in computer vision applied in smart farms in still an open research. In this paper, scale invariance was addressed by detecting markers with known size and components for normalizing area measurements. This study demonstrated the effectiveness of the automated object detection (marker) with limited training samples using Viola-Jones algorithm that uses Haar-like, HOG and LBP features. Performances of the system using each feature at varying illuminations and capture distances were also compared. Based on the result of this study the best performance in object (marker) detection in general, based on accuracy, precision, and false positive rate is achieved using HOG features. Though most of the markers are detected using any feature, there is a high occurrence of false positives. It is recommended for future work therefore to introduce another algorithm to address the filtering out of false positives. To minimize the amount of false positive detections, the models can be refined by adding knowledge-based algorithms corresponding to the unique image features of the markers such as color, corners and number of connected objects.

Acknowledgment

The authors would like to extend their gratitude to the USAID STRIDE, Department of Science and Technology – Philippine Council for Industry, Energy and Emerging Technology Research and Development (DOST-PCIEERD) and Commission on Higher Education (CHED) for the financial support in this research. Also, special thanks to the Intelligent Systems Laboratory for allowing the authors to use their laboratory equipment and project site in the completion of this study.

References

[1] R. K. Kodali, V. Jain and S. Karagwal, "IoT based smart greenhouse," in *Proceedings of 2016 IEEE Region 10 Humanitarian Technology Conference (R10-HTC)*, 2016. https://doi.org/10.1109/R10-HTC.2016.7906846.

[2] F. Xinyan, K. Kensuke, G. Wei, D. X. Tran, L. Jihyun, Y. Norio, K. Yuzo, O. Taketo, L. Renlong, T. Yoshimasa, Y. Taisuke and W. Zuomin, "A simple visible and near-infrared (V-NIR) camera system for monitoring the leaf area index and growth stage of Italian ryegrass,," *Computers and Electronics in Agriculture*, vol. 144, pp. 314-323, 2018. https://doi.org/10.1016/j.compag.2017.11.025.

[3] A. Rajput, S. Rajput and G. Jha, ""Physiological Parameters Leaf Area Index, Crop Growth Rate, Relative Growth Rate and Net Assimilation Rate of Different Varieties of Rice Grown Under Different Planting Geometries and Depths in SRI,"," *International Journal of Pure and Applied Bioscience*, vol. 5, no. 1, pp. 362-267, 2017. https://doi.org/10.18782/2320-7051.2472.

[4] Q. Xie, W. Huang, D. Liang, P. Chen, C. Wu, G. Yang, J. Zhang, L. Huang and D. Zhang, "Leaf Area Index Estimation Using Vegetation Indices Derived from Airborne Hyperspectral Images in Winter Wheat," *IEEE Journal of Selected Topics in Applied Earth Observations and Remote Sensing*, vol. 7, no. 8, pp. 3586-3594, 2014. https://doi.org/10.1109/JSTARS.2014.2342291.

[5] R. R. Fang Y., "Current and prospective methods for plant disease detection," *Biosensors*, vol. 5, no. 3, pp. 537-561, 2015. https://doi.org/10.3390/bios5030537.

[6] D. Fernandez-Pacheco, D. Escarabajal-Henarejos, A. Ruiz-Canales, J. Conesa and J. Molina-Martinez, "A digital image-processing-

based method for determining the crop coefficient of lettuce crops in the southeast of Spain," *Biosyst. Eng*., vol. 117, pp. 23-34, 2014. https://doi.org/10.1016/j.biosystemseng.2013.07.014.

[7] N. Bumgarner, W. Miller and M. Kleinhenz, "Digital image analysis to supplement direct measures of lettuce biomass," *HortTechnology*, vol. 22, no. 4, pp. 547-555, 2012. https://doi.org/10.21273/HORTTECH.22.4.547.

[8] C. Shi-Gang, L. Heng, W. Xing-Li, Z. Yong-Li and H. Lin, "Study on segmentation of lettuce image based on morphological reorganization and watershed algorithm," *Proceedings of 2018 Chinese Control and Decision Conference (CCDC)*, 2018. https://doi.org/10.1109/CCDC.2018.8408290.

[9] P. Srivastava & A. Khare "Content-based image retrieval using scale invariant feature transform and moments", *Proceedings of 2016 IEEE Uttar Pradesh Section International Conference on Electrical, Computer and Electronics Engineering (UPCON)*, pp. 162 – 166, 2016. https://doi.org/10.1109/UPCON.2016.7894645.

[10] W. G. Aguilar, M. A. Luna, J. F. Moya, V.Abad, H. Parra, H. Ruiz, "Pedestrian detection for UAVs using cascade classifiers with meanshift", *Proceedings of 2017 IEEE 11th International Conference on Semantic Computing*, 2017. https://doi.org/10.1109/ICSC.2017.83.

[11] M. Nehru & S. Padmavathi, "Illumination invariant face detection using viola jones algorithm", *Proceedings of 2017 4th International Conference on Advanced Computing and Communication Systems (ICACCS)* , pp. 1-4, 2017. https://doi.org/10.1109/ICACCS.2017.8014571.

[12] D. Djamaluddin et. al, "The simulation of vehicle counting system for traffic surveillance using Viola Jones method", 2014 Makassar *Proceedings of International Conference on Electrical Engineering and Informatics (MICEEI)*, pp. 130-135, 2014. https://doi.org/10.1109/MICEEI.2014.7067325.

[13] A. Anchit & S. Mathur, "Comparative analysis of Haar and Skin color method for face detection", *Proceedings of International Conference on Recent Advances and Innovations in Engineering (ICRAIE-2014)*, pp. 1 – 5, 2014. https://doi.org/10.1109/ICRAIE.2014.6909143.

[14] M. Sonka, V. Hlavac,, R. Boyle, *Image Processing, Analysis, and Machine Vision*, Cengage Learning, pp. 509-510, 2015.

[15] M. Sonka, V. Hlavac, R. Boyle, *Image Processing, Analysis, and Machine Vision*, Cengage Learning, pp. 757-759, 2015.

[16] Heirloom, ""How to Grow Loose Leaf Lettuce,"," 2017. Available online: http://www.heirloomorganics.com/guide/va/1/guidetogrowinglooseleaflettuce.html. last visit:18.01.2019.

[17] S. Ervural and M. Ceylan, "Increasing lesion specificity with fusion of manually and automatically segmented liver MR images," *Proceedings of* 2018 *26th Signal Processing and Communications Applications Conference (SIU)*, 2018. https://doi.org/10.1109/SIU.2018.8404559.